Marine Pollution Bulletin 207 (2024) 116842

Contents lists available at ScienceDirect

Marine Pollution Bulletin

journal homepage: www.elsevier.com/locate/marpolbul

Experimental detection of marine plastic litter in surface waters by 405 nm LD-based fluorescence lidar

Jumar Cadondon [a,b,*], Edgar Vallar [a], Tatsuo Shiina [c], Maria Cecilia Galvez [a]

[a] Environment And RemoTe sensing researcH (EARTH) Laboratory, Department of Physics, College of Science, De La Salle University Manila 0922, Philippines
[b] Division of Physical Sciences and Mathematics, College of Arts and Sciences, University of the Philippines Visayas, Miagao 5023, Iloilo, Philippines
[c] Graduate School of Science and Engineering, Chiba University, Chiba-Shi, Chiba 263-8522, Japan

ARTICLE INFO

Keywords:
Fluorescence
Lidar
Plastic litter
Microalgae
Chlorophyll
Water pollution
Weathering

ABSTRACT

Plastic pollution has become a global challenge, affecting water quality and health. Plastics including polystyrene (PS), polyvinyl chloride (PVC), polypropylene (PP), polyethylene terephthalate (PET), and high-density polyethylene (HDPE), are significant contributors to environmental pollution. With the growing need for investigation and detection of plastics found in natural waters, we propose the use of a portable laser diode (LD)-based fluorescence lidar system for in-situ detection of plastic litters in surface waters based on excitation-emission fluorescence spectroscopic data. The experiments were carried out in a controlled environment using a fluorescence lidar system with 405 nm excitation wavelength to determine the fluorescence signals of several plastics at 470 nm emission wavelength. Simultaneous detection of PET plastic and *Chlorella vulgaris* were also observed to determine the fluorescence influence of chlorophyll in surface waters. Attenuated total reflection Fourier transform infrared (ATR-FTIR) spectroscopy was employed to study the chemical composition of the plastics used before and after being submerged in the water. Scanning electron microscopy (SEM) and high-resolution camera microscopy were used to analyze the morphology of the submerged PET samples. This study provides a basis for a new in-situ technique using a fluorescence lidar system for submerged or transparent plastics in surface waters.

1. Introduction

Plastic pollution caused by industrialization, agricultural production, and urban activities affects water quality in oceans, lakes, and rivers (Lin et al., 2022; MacLeod et al., 2021; WHO, 2019). Plastic pollutants from different sources significantly contribute to poor water quality when released into water systems, affecting human health and sustainable development. One emerging pollutant that has attracted the research community is the growing detection of marine plastic litter (MPL) in the ecosystem (Strand et al., 2021; Mallory et al., 2021). The fraction of all the plastics produced and used are leaked into the world's oceans, which vary according to sizes such as megaplastics (>1.0 m), macroplastics (25–1000 mm), mesoplastics (25–1000 mm), and microplastics (1–5000 μm) (Rapa et al., 2024). Plastic contamination in marine environments is widely studied, but detection in freshwater bodies is gaining attention. Freshwater systems are drinking water sources for irrigation and link land-based MPL sources to marine environments (Wagner et al., 2014).

The current detection for MPL mainly includes microscopy (visual microscope and scanning electron microscope) (Loder and Gerdts, 2015; Armitage et al., 2022), Fourier infrared spectroscopy (Mikulec et al., 2023), fluorescence imaging (Wohlschlager and Versen, 2020; Zhou et al., 2022), and thermal pyrolysis analysis (Mai et al., 2018). Specific protocols must be followed in processing and preparing environmental plastic contamination before it can be quantified and characterized. Visual inspection is the most convenient and cheap protocol that can provide the physical properties of plastics (Vianello et al., 2013). Spectroscopic methods are used to compare collected data with a reference to provide information on plastic samples. However, these methods require water sampling and are unsuitable for in situ detection.

Recent studies show that the remote sensing technique is a promising tool for application to plastic detection and characterization (Martinez-Vicente et al., 2019; Mace, 2011; Maximenko et al., 2019). These techniques have already been observed in experimental studies under controlled environments, and some conducted in field monitoring using different platforms or instruments (Garaba et al., 2018; Goddijn-Murphy

* Corresponding author at: Division of Physical Sciences and Mathematics, College of Arts and Sciences, University of the Philippines Visayas, Miagao 5023, Iloilo, Philippines.
E-mail address: jgcadondon@up.edu.ph (J. Cadondon).

https://doi.org/10.1016/j.marpolbul.2024.116842
Received 3 June 2024; Received in revised form 7 August 2024; Accepted 9 August 2024
Available online 21 August 2024

et al., 2018; Park et al., 2021; Evans and Ruf, 2021; Geraeds et al., 2019). With the growing number of studies and experiments using passive techniques such as fluid sensing, multi-angle polarimetry, thermal infrared sensing, and active techniques (Goddijn-Murphy et al., 2024), there are still limited reports on the potential use of light detection and ranging (Lidar) techniques for the remote sensing of plastic debris (Palombi and Raimondi, 2022). Lidar techniques are developed for atmospheric studies and aquatic environments (Measures, 1984). Fluorescence Lidar systems, a type of remote sensing technique, provide information on the optical properties that can be observed in freshwater systems such as colored dissolved organic matter (CDOM), phytoplankton, and other pollutants (Rogers et al., 2012; Palmer et al., 2013; Cadondon et al., 2022; Cadondon et al., 2023; Saito et al., 2014; Churnside and Thorne, 2005). There are ongoing efforts to develop novel spaceborne lidar missions for oceanographic applications. Nonetheless, fluorescence lidar experiments on plastic litters in algae-plastic scenarios have yet to be conducted.

1.1. Plastics and phytoplankton in the environment

Several studies have proven they can carry pathogens that lead to human infection (Meng et al., 2021). Other than suspended particles observed on the plastics' surface, direct contact with pathogen-colonized plastics may cause contamination (Pang et al., 2020; Hale and Song, 2020).

Plastic marine debris has been studied as a habitat for microbial biodiversity in changing marine ecosystems (Dussud et al., 2018). The increased plastic concentration changes zooplankton populations, leading to an imbalance in the marine nutrients and carbon cycles (Galgani and Loiselle, 2021). The interaction of microorganisms with plastics caused by microbial colonization of floating plastic surfaces is accountable for surface biofilm formation (Casabianca et al., 2021). The potential interactions between plastic polymers and phytoplankton assemblages are discussed in this study, along with the system's capability of simultaneous detection of plastics and chlorophyll-a. However, there is still a need for future research on the occurrence and distribution of smaller plastic debris along the water column and bottom sediments using a remote sensing system. Standardization of methods used for laboratory and in-field measurements needs to be carried out to provide guidelines that the scientific community can share.

This study gives information on the first fluorescence lidar data of commonly used plastics submerged in surface water systems. The following objectives are: (1) to compare the fluorescence emission of several plastics using EEM fluorescence spectroscopy and (2) to detect MPL using the developed portable LD-based fluorescence lidar system. This study can provide information on the interaction of plastics and phytoplankton community in surface waters, which can be improved in future research. This study is a good reference supporting the call of the World Health Organization (WHO) to report the presence of MPL and the emergence of microplastics, which affect human health and the environment (WHO, 2019).

1.2. Theory

1.2.1. Fluorescence

Fluorescence is the emission of photons from a sample following the absorption of photons (Povrozin and Barbieri, 2016). The Jablonski diagram illustrates the processes that occur between the absorption and emission of light. The ultraviolet and visible regions of the spectrum are commonly used in fluorometry and absorption since these regions cause the excitation of the outermost electrons of the molecule. Light absorption in these regions forms excited molecules, which can dissipate their energy through different processes such as decomposition, reaction, or re-emission (Bassi and Dall'Osto, 2021). Any photon with an excitation wavelength of 370 to 690 nm that is absorbed produces fluorescence. The redistribution function of the fluorescence wavelength can be written as:

$$f_f(\lambda) = \Phi_f g_f(\lambda') h_f(\lambda) \frac{\lambda'}{\lambda} \tag{1}$$

where Φ_f is the quantum efficiency for fluorescence, it is the ratio of the photons absorbed at a given wavelength and the total number of photons emitted at all wavelengths. The reported average value of Φ_f in surface waters is 0.07 (Falkowski et al., 2017). $g_f(\lambda')$ is the interval over which light can excite fluorescence defined by a step function, and $h_f(\lambda)$ is the fluorescence wavelength emission function defined by the Gaussian function (Santabarbara et al., 2020) given by

$$h_f(\lambda) = \frac{1}{\sigma_c\sqrt{2\pi}} exp\left[-\frac{(\lambda-\lambda')^2}{2(\sigma_c)^2}\right] \tag{2}$$

where λ' is the wavelength of maximum emission and σ_c is the standard deviation of the Gaussian, which is related to the full width-half maximum (FWHM) of the fluorescence excitation spectrum (Chen et al., 2023) given by

$$\sigma_c = FWHM \Big/ 2\sqrt{2ln2} \tag{3}$$

In this study, the optical properties of microalgae, MP, and CDOM were classified, and bio-optical models were used (Table A.1). The absorption and scattering coefficients (Shangguan et al., 2024) are modeled as follows:

$$a(\lambda) = a_w(\lambda) + a_{MP}(\lambda) + 0.06\, a_c^{*'}(\lambda) + a_y(\lambda) \tag{4}$$

$$b(\lambda) = b_w(\lambda) + b_{MP}(\lambda) + b_P(\lambda) \tag{5}$$

where a_w is the absorption coefficient of pure water, $a_c^{*'}$ is the normalized spectral absorption values of phytoplankton pigments, a_y is the absorption coefficient of organic matter distribution, a_{MP} is the absorption coefficient of the induced microplastics, b_w is the scattering coefficient of water, b_{MP} is the scattering coefficient of marine plastics, and b_P is the scattering coefficient of phytoplankton. In this study, the phytoplankton pigment measured is the chlorophyll concentration measured at 680 nm.

2. Materials and methods

2.1. Sample preparation

In this work, pure (Sanei Chemical Co., Ltd., Arao, Japan) and pond water samples, plastic samples (NaRiKa Co., Ltd., Tokyo, Japan), and *Chlorella vulgaris* (*C. vulgaris*), a green alga, were prepared. Fig. 1(C) and Table 1 shows the plastic samples selected for the experiment. Pond samples were collected in Katarai no Mori Park, Chiba University, Nishi-Chiba Campus, Chiba, Japan (35° 37′ 37.542″ N, 140° 6′ 10.2996″ E). *C. vulgaris* was cultured at 2000 lx light intensity with a 12 h/12 h light/dark cycle using a BG-11 culture medium.

All measurements were carried out on plastic samples immersed in the water (Fig. 1(C)); we used a 29-L glass tank (30 cm × 30 cm × 35 cm) that allowed us to simulate the effect of different water samples. This setup was adopted to reproduce realistic experimental conditions in which the laser beam is attenuated by the water column and some major fluorescence contributors, such as CDOM and phytoplankton pigments.

2.2. Excitation-emission matrix (EEM) analysis

Using an excitation-emission spectroscopy setup, dry and wet plastic samples' fluorescence emission is studied using a 10 mm cuvette. For the wet conditions, plastic samples were submerged in pure water. In this study, the excitation wavelength is 405 nm with an uncorrected fluorescence spectrum ranging from 200 to 2000 nm. In this experiment, the

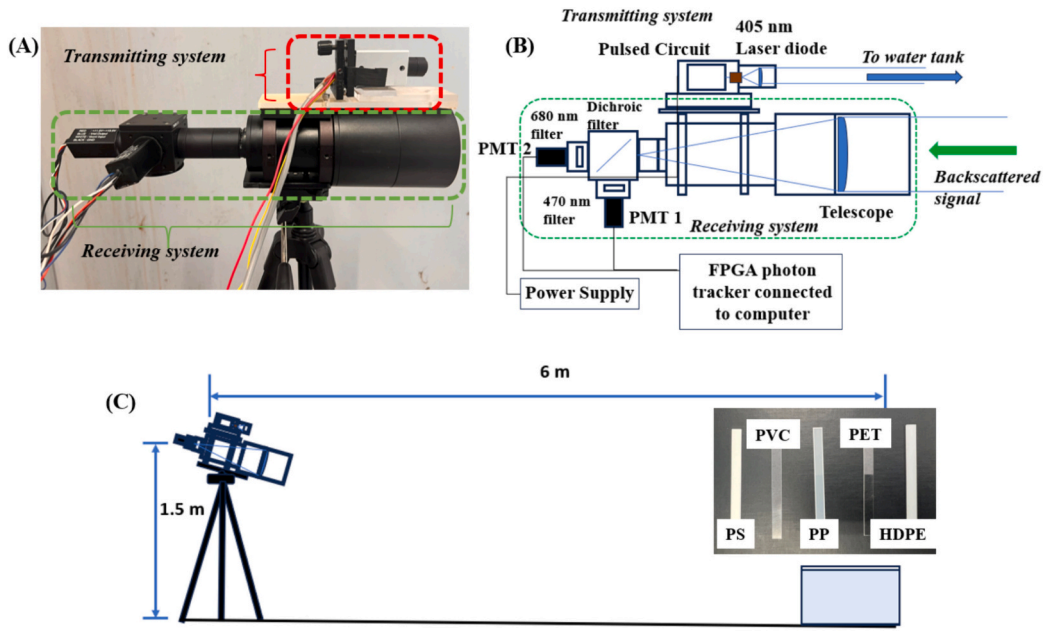

Fig. 1. (A) Actual fluorescence lidar system, (B) schematic diagram, and (C) experimental setup and plastic samples used in the laboratory for the fluorescence lidar measurements.

Table 1
Description of typical plastic samples used (NaRiKa, n.d.).

Material	Code	Mass (g)	Specific gravity	Common uses
Polypropylene	PP	1.22	0.90	Kitchen utensils, films, containers
Polystyrene	PS	1.31	1.05	Transparent daily necessities, containers, stationery, highly foamed products
Polyvinyl chloride	PVC	1.67	1.45	Agricultural films, pipes, hoses, electrical wire coatings
Polyethylene terephthalate	PET	1.62	1.55	Bottles, Home appliance parts, recording tapes
High-density polyethylene	HDPE	1.27	0.95	Packaging films, laminates, toys, daily necessities

spectral range studied for the fluorescence of plastic samples ranges from 450 to 700 nm. For the data acquisition, the signal from the spectrometer was set to 10,000 calibration offsets, and the saturation level was 5000. The scans to average per sample were set to 10 with a box scar width of 3. The integration time is approximately 0.4 min. Ten (10) blank cuvettes were used for the dry samples to measure the background signal before adding the plastic samples. Raw fluorescence spectra of dry plastic samples were measured and recorded. Fifty (50) pure water samples served as blank samples for the submerged plastic samples. The plastic samples were submerged into the pure water samples and were analyzed for fluorescence emissions. In this experiment, the raw fluorescence signal is processed by subtracting the blank samples and using Fast Fourier Transform (FFT) algorithm to gather the corrected fluorescence signal (Cadondon et al., 2022; Cadondon et al., 2023).

2.3. Development of the fluorescence lidar system

The portable fluorescence lidar system uses a 405 nm laser diode (LD) (Thorlabs L405P20) as a light source. It comprises a transmitter, a receiver, and a signal processing unit (Fig. 1(A)). The LD is part of the transmitting system, which allows pulsed modulation at a very low voltage input. It consists of a pulsed driver circuit with trigger control, as shown in Fig. 1(B). The same pulsed circuit was used as presented previously with minor electronic modifications. The maximum output power of the transmitting system after collimation is 0.45 W, which enables the detection of small particles at low concentrations. The receiving system utilizes an assembled refracting telescope with an aperture of 75 mm. An iris is placed at the telescope's focal point before the fluorescence filters to measure the scattering volume. The scattering volume is defined as the intersection of the incident light and the detected volume. The laser's diameter is approximately 1 cm, smaller than the telescope's beam divergence. A multi-edge dichroic mirror separated signals from the CDOM and chlorophyll. It has a 100 % reflectance for 450 to 500 nm and a 100 % transmittance for 500 to 700 nm. CDOM and plastic samples were measured at 470 nm with a fluorescence bandpass filter. On the other hand, the chlorophyll detection was measured at 680 nm with a fluorescence bandpass filter.

The developed lidar system has a biaxial configuration. The transmitting and receiving components were aligned to optimize the backscattered signal to provide maximum fluorescence intensity at a chosen distance. This concept proves the feasibility of 180° fluorescence detection of plastic samples, as previously discussed (Palombi and Raimondi, 2022; Shangguan et al., 2024). With this setup, the maximum backscattered light can be improved by proper alignment, which depends on the position of the samples. It optimizes the fluorescence lidar signal that the photomultiplier tube (PMT) can detect. The intensity of the backscattered signals was measured using a PMT with a wavelength range from 185 to 870 nm. The photocathode area size has a diameter of 8 mm. This photomultiplier tube delivers high gain, wide dynamic range, and high-speed response and is designed for photon counting. It can measure low-scattering signals emitted from photons observed by the receiving system. For signal processing, an FPGA-based photon counting board (Trimatiz Co., Ltd., Photon Tracker, Chiba, Japan) was developed (Shiina, 2019). It has a four-channel input for multiple-channel detection, with a system clock of 500 MHz with 2 W for each channel. The highest resolution has a BIN width of 5 ns, with a range resolution of 0.75 m and a minimum summation time for data transfer of 0.2 s. The configuration of the portable LD fluorescence lidar system is provided in Fig. 1(C), with the technical specifications reported in Table 2.

Table 2
Technical specifications of the LD-based fluorescence lidar system.

Components	Parameter	Value
Laser diode	Central wavelength	405 nm
	Pulse width	11 ns
	Divergence angle	0.5 mrad
Telescope	Diameter	75 mm
	Field of view	~2 mrad
Detection device	PMT: Hamamatsu H11901P-10	185–870 nm
Dichroic mirror	Reflectance	400–500 nm
	Transmittance	500–700 nm
Filters	Plastic signal	470 nm
	Chl-a	680 nm
Photon counter	FPGA photon tracker	
	System clock:	550 MHz
	BIN Width	5 ns
	BIN length	50

2.4. Spectral processing and analysis

Backscattered lidar signals was measured based on the FPGA photon counter. Using such a photon counting device with its overall built assembly helps improve data collection, strong real-time preformation, and high integration. A database was created, which consists of the following: (a) pure, freshwater (pond), and seawater samples; and (b) *C. vulgaris* concentrations. Several couples of active/background measurements are acquired to increase the signal-to-noise ratio (SNR) to obtain the backscattered fluorescence lidar signal of water samples. The data collected from these water samples, $b_w(\lambda)$, served as blank samples. All succeeding fluorescence spectra, $b(\lambda)$, were corrected based on the spectral response from the different water samples, and estimation algorithms such as the convex hull algorithm, Gaussian fitting with the Levenberg Marquardt method, and the FFT algorithm were used. The maximum fluorescence peak signal is then obtained for each spectrum.

2.5. Chemical and morphological analyses

Attenuated total reflection Fourier transform infrared (ATR-FTIR) spectroscopy (Agilent Cary 630, CA, USA) was employed to PET samples before and after submerged in water. The nominal spectral resolution is 8 cm^{-1} within the 4000–500 cm^{-1} range. A collection time of 15 s was used for each measurement, with an average scan of 40. Morphological characterizations were also conducted in all PET samples using a field emission scanning electron microscope (FE-SEM), as discussed previously (Cadondon et al., 2024). For lower-resolution images, a high-resolution microscope (Axios microscope coupled with Wraymer high-resolution camera) was used to identify suspended particles after being submerged in pond water.

3. Data and results

In this study, preliminary experiments of the samples were analyzed using excitation-emission spectroscopy. Based on the excitation-emission pairs collected, the pulsed LD-based fluorescence lidar system was developed for fluorescence detection of several plastic litters. We also provide information on the plastic litter affected by the chlorophyll distribution of microalgae in surface waters.

3.1. Excitation-emission pairs of different plastic samples

Dry and submerged samples of several plastics were carried out using spectroscopy. The collected information on the fluorescence spectra of several plastic litters is provided in Fig. 2. The spectra acquired use a 405 nm excitation wavelength and emission wavelength spectrum from 420 nm to 700 nm at room temperature. All fluorescence spectra are measured in arbitrary units (a.u.) with ten scans to average. The detectable fluorescence spectrum ranges from 450 to 700 nm. The fluorescence spectra below 450 nm are affected by the spectrum of the excitation wavelength. With the subtraction of the background signals, environmental factors and internal noises in the photon counting device are reduced. On the other hand, the fluorescence spectral shape of the different plastic litters remains unchanged even after being submerged. The big difference in the absorbed photons (Fig. 2(A, D, E)) at 450 to 600 nm shows a higher absorption rate of PS, PET, and HDPE. EEM pairs of measured plastics have been observed previously (Maslov and Dulin, 2020). Even without fluorescent colorants commonly used in plastics, high fluorescence intensity is observed in PET samples (Lionetto et al., 2020).

Fig. 3 shows the mean distribution of dry and submerged plastic samples. Higher fluorescence emission is observed when the plastic samples are submerged. The same increase in the fluorescence intensity has been observed when measured at 470 nm and 525 nm. PS, PP, PET, and HDPE plastics showed two folds or more in the fluorescence intensity when submerged. When submerged, this high light absorption by water increased substantially with the plastics' reflectance signals. The comparison of the fluorescence signals using the chosen two-wavelength measurements provided significant differences for dry and submerged plastics.

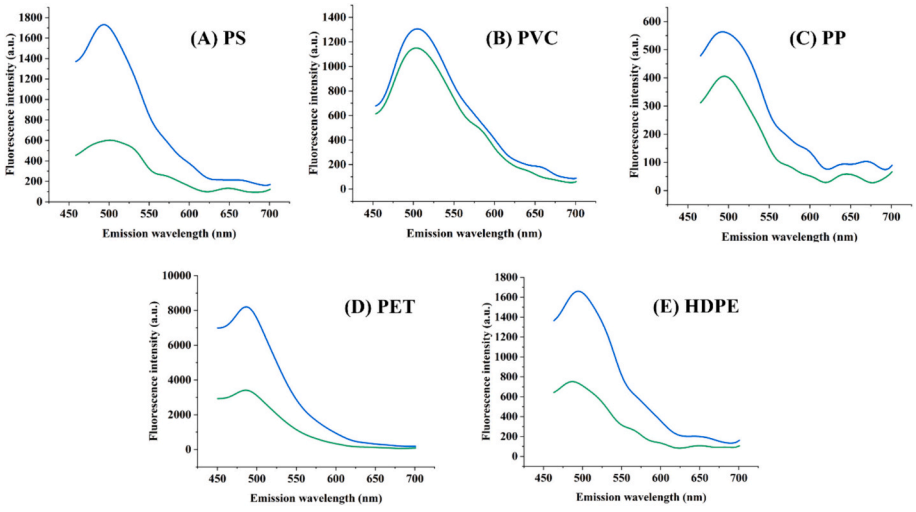

Fig. 2. Fluorescence spectra of several plastics using excitation-emission spectroscopy. The green line represents the dry samples, while the blue line represents the submerged samples. (For interpretation of the references to color in this figure legend, the reader is referred to the web version of this article.)

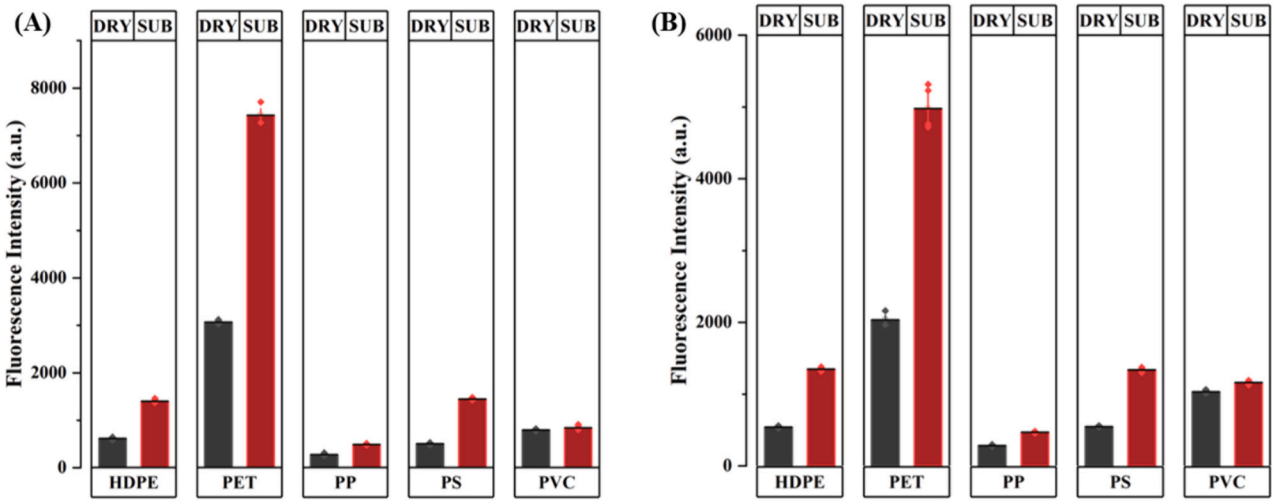

Fig. 3. Box plot of EEM fluorescence signals at (A) 470 nm and (B) 525 nm. DRY represents the dry plastics and SUB represents the submerged plastics.

3.2. *Fluorescence lidar measurement of plastics in surface waters*

From the corrected fluorescence EEM, several peaks were chosen for plastic detection. Emission wavelengths at 470 nm and 525 nm were used to compare the fluorescence spectra of several plastics using the fluorescence lidar system (Fig. A.1). Fluorescence lidar signal measurements of pure, fresh, and marine waters were analyzed. Experiments were performed in a dark environment to minimize dark noises from the background. The threshold level was set at −20 mV with a fall slope. The fluorescence contribution of the black sheet is negligible, and the fluorescence intensity is the same when the receiving component of the lidar system is covered. The fluorescence lidar signal of several water samples varies (Fig. A.2). The fluorescence intensity is dependent on the water sample, with higher intensity measured at 470 nm compared to 525 nm. Signal-to-noise (SNR) ratio also showed that marine waters have higher SNR than fresh and pure waters. Possible noises observed can be attributed to organic matter distribution and several suspended particles found in fresh and marine water samples.

The first part of the fluorescence lidar experiment was carried out on the plastics submerged 10 cm below the water's surface in the water tank. The distance between the lidar system and the water tank is 6 m. It simulates the average distance from the riverbanks to surface waters. At this distance, the area on the target seen by the lidar is a 1 cm diameter spot size. At shallow angle measurements (0–5°), the interaction between the lidar signal and the water-plastic scenario can be captured (Shiina, 2020). Fig. 4 shows all the fluorescence lidar signals acquired on the different plastic samples submerged in pure and fresh (pond) waters. All fluorescence signals of the plastic litter were observed with the PET sample with the highest intensity on both emission wavelengths. Lower fluorescence signals are observed in PP and PS samples, which exhibit their dependence on excitation-dependent fluorescence characteristics (Zhao et al., 2022). We subtracted the raw fluorescence signal collected to remove the water Raman contributions and organic matter distribution in water samples (Palombi and Raimondi, 2022). The subtraction method has been applied to all raw fluorescence spectra for both emission wavelengths. The intensity of all corrected fluorescence signals has decreased primarily because of water Raman and organic matter. Fig. 4 (B) shows the fluorescence lidar signal measurements of plastics when submerged in pond waters. The fluorescence peak signal of all plastics is maintained after being submerged in the pond water tank. However, the fluorescence lidar signals of plastic samples are dominant, and the changes in water samples are relatively trivial. Corrected peak fluorescence signals of plastics using pure and pond waters showed no significant difference (Fig. A.3), but higher peak signals were detected in pond waters.

With the unique design of the receiving component of the fluorescence lidar system, simultaneous detection of plastic litter and microalgae is possible. *C. vulgaris* was added to investigate the feasibility of distinguishing plastics. We have previously reported chlorophyll- a measurement of several microalgae using a portable LED fluorescence lidar system with an excitation wavelength of 385 nm and emission (fluorescence) wavelength of 680 nm. It can be observed that the EEM of CDOM is also observed at 405 nm excitation wavelength (Cadondon et al., 2022).

The fluorescence band can quickly identify fluorescence contributions from phytoplankton due to chlorophyll in the red region. This can

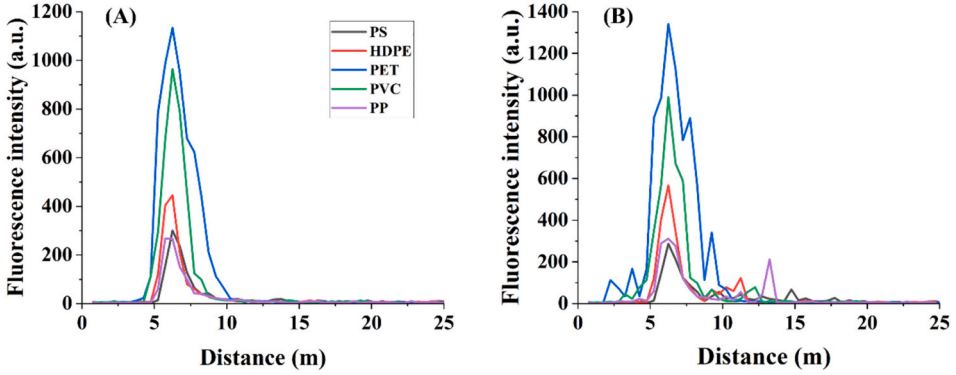

Fig. 4. Fluorescence lidar signal of plastic samples submerged in (A) pure water and (B) fresh (pond) water.

be extended in understanding behaviors of several natural water debris, such as leaves and algae, which are common suspended particles (Palombi and Raimondi, 2022; Cadondon et al., 2022; Cadondon et al., 2023; Falkowski and Kolber, 1995). The fluorescence CDOM lidar signal of *C. vulgaris* at 470 nm was measured and subtracted to measure the fluorescence lidar signal of the plastic samples. The fluorescence intensity is still relatively small compared to the fluorescence intensity of the plastic samples. Overall, the fluorescence intensity of CDOM increases with increasing biomass concentration. To further understand the relationship between phytoplankton and plastic litter, simultaneous detection was conducted using 470 nm and 680 nm for plastic litter and chlorophyll-a, respectively. Fig. 5 shows the fluorescence lidar signal of the PET plastic with *C. vulgaris.* The fluorescence lidar signal of PET samples showed a widening signal when *C. vulgaris* was added. It can be observed that the chlorophyll fluorescence signal increases with its biomass concentration ($R^2 = 0.97$, $p < 0.05$). On the other hand, the fluorescence signal at 20 mg/L *C. vulgaris* biomass is relatively similar with 25 mg/L concentration. It tells us that the maximum detection of the fluorescence lidar system is approximately equal to 20 mg/L. The fluorescence emission of vegetation is characterized by two fluorescence bands, 680 nm, and 740 nm, tightly linked to photosynthesis. This study used one of the two photosynthetic bands to estimate chlorophyll-a concentration. With the addition of increasing algal biomass, we could detect the PET sample's fluorescence signal. These results show that our system can effectively provide fluorescence information on plastic litter and microalgae in surface waters.

The fluorescence emission of plastic litter used in this study was analyzed using excitation-emission spectroscopy and the developed fluorescence lidar system. Correlation analysis was computed from the fluorescence intensities observed. The corrected fluorescence lidar signal and EEM fluorescence signal showed positive correlation for PP ($R^2 = 0.76$, $p < 0.05$), PVC ($R^2 = 0.64$, $p < 0.05$), PS ($R^2 = 0.82$, $p < 0.05$), HDPE ($R^2 = 0.88$, $p < 0.05$), and PET ($R^2 = 0.90$, $p < 0.05$) measured at 405 nm excitation wavelength and 470 nm emission wavelength. This implies that the portable LD-based fluorescence lidar system can detect plastic in surface waters, as supported by EEM fluorescence data.

3.3. Weathering of plastic litters

In a natural environment, organic matter and some detritus, such as MPL, change due to electromagnetic radiation, biochemical processes, and climatic effects. The second part of the experiment is to simulate the effects of the natural environment on plastic samples. PET plastics were submerged during the fall (October and November 2023), winter (February 2024), and spring (May 2024) seasons in a pond inside Chiba University. Under different climatic conditions, pond water samples and submerged PET plastic were collected and analyzed for lidar measurements. Fluorescence lidar observation during nighttime showed consistent measurements of MPL with varying seasons (Fig. 6), confirming real-time data collection of the system. Chlorophyll-a (μg/L) measurements, weather data such as air and water temperature (°C), and relative humidity (%) were also measured. MPL detection at varying seasons showed consistent fluorescence signals with higher SNR measurements during winter after eight months.

The observed increase in SNR is explained by the possible interaction of suspended particles found in the plastic's surface (Fig. 7A). It is supported by the FTIR images before and after being submerged (Fig. 7B). Surface characterization (Fig. 7C) through SEM showed physical breaking (Ashjar et al., 2023). FTIR images showed a typical spectrum of PET, such as 1111 cm^{-1} for asymmetrical C-O-C stretching and 518–875 cm^{-1} indicative of an aromatic ring (Alzhuhairi et al., 2016; Circelli et al., 2024). EDS results of PET samples collected in October 2023 showed a high carbon content with a 97.23 mass percentage. Carbon, oxygen, sodium, and silicon particles are found on the PET's surface after being submerged for eight months (Fig. A.3). These particles are

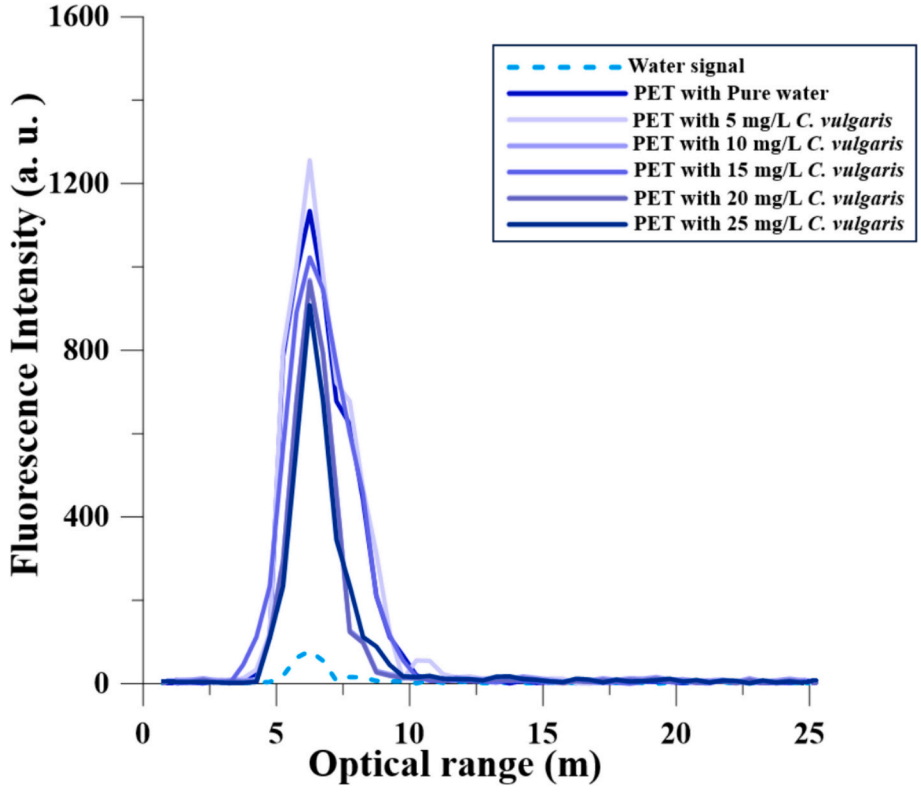

Fig. 5. Fluorescence lidar signal of PET plastic with varying *C. vulgaris* biomass concentration. Fluorescence lidar signal of water and PET submerged in pure water as references.

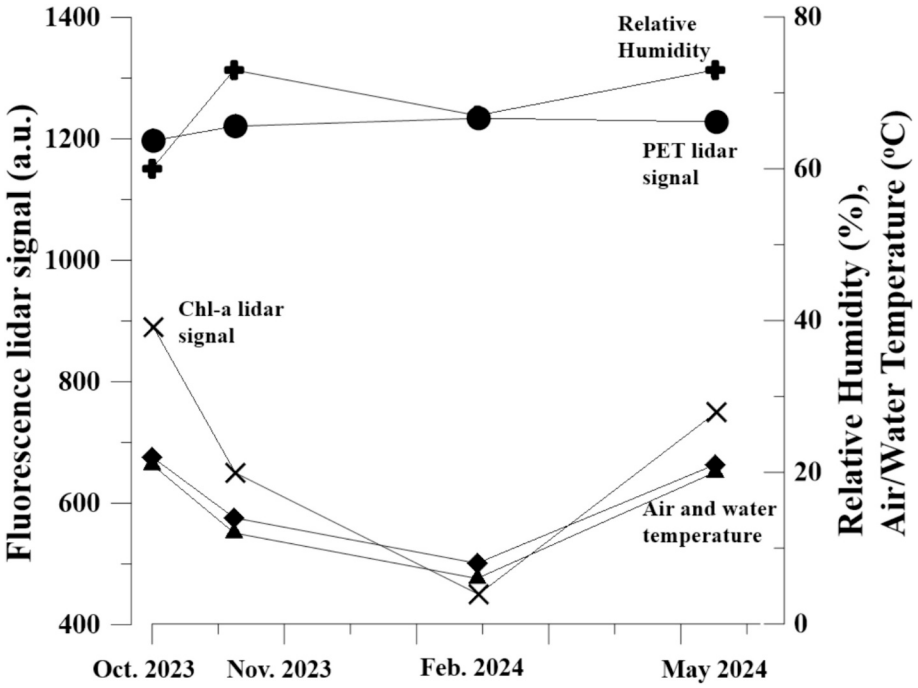

Fig. 6. Seasonal variations of PET plastic, weather parameters, and chlorophyll signal.

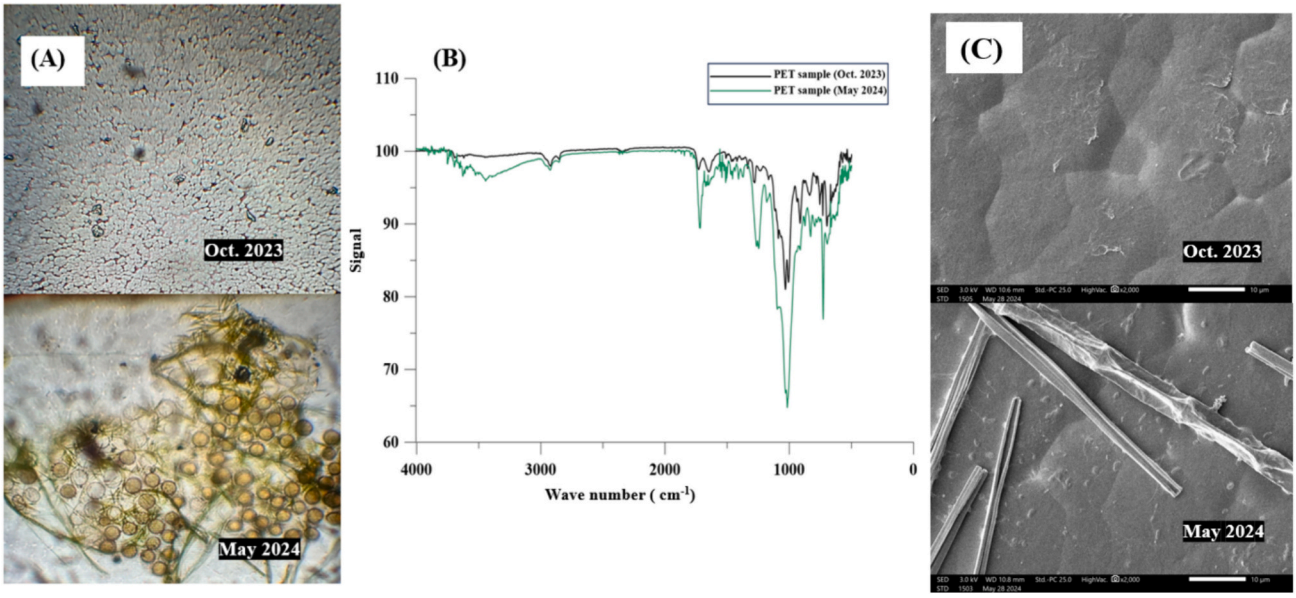

Fig. 7. (A) High-resolution images, (B) FTIR spectra, and (C) SEM images of PET plastics' surface measured in October 2023 and May 2024.

commonly observed for suspended objects on plastic surfaces.

4. Discussion

4.1. Fluorescence patterns of plastics due to water and climate conditions

Plastic litter is a growing environmental issue on a worldwide scale threatening marine ecology and the society. Plastic materials have poisonous compounds when polymers undergo degradation. Photodegradation is mainly responsible for the initial degradation of plastics in surface waters, while biodegradation by microorganisms in biofilms is the leading cause of plastic degradation (Duan et al., 2021). This study presents the use of a fluorescence lidar system in detecting the early degradation of plastics in surface waters.

Most of the studies on detecting and mapping MPL consider either beached or floating objects (Andriolo et al., 2020; Goddijn-Murphy et al., 2018; Maximenko et al., 2019), and studies on submerged or underwater detection is still unaccounted. The developed fluorescence lidar system effectively detects submerged plastic debris in a small-scale scenario. Plastic materials do not have standard parameters, such as shape, dimension and chemical composition (Veettil et al., 2022). Any qualitative and quantitative characteristic of plastic litter must be used to distinguish it from other materials. It was found out that the fluorescence spectra of several plastics (PS, PP, PVC, PET, HDPE) are maintained even when submerged (Fig. 2). Fluorescence lidar signals of plastics submerged in pure water showed smooth patterns (Fig. 4(A)).

The change in water samples showed noisy spectra but the peak fluorescence signal is maintained (Fig. 4(B)). They are affected by suspended particles observed in the water column which causes turbidity. The introduction of increasing *C. vulgaris* concentrations simulates the turbidity in water. Fig. 5 shows the constant fluorescence lidar signals as the *C. vulgaris* concentration increases. With the changing climatic conditions observed, integration of several weather and water quality parameters with the aid of a fluorescence lidar system allows complete understanding of plastic behavior in water systems.

4.2. Fluorescence lidar systems for plastic litter and phytoplankton monitoring

Plastics exhibit unique spectral characteristics that set them from natural materials, forming the basis for detections using remote sensing applications (Mahmoud and El-Sharkawy, 2024). Different types of plastics exhibit fluorescence responses (Fig. 2), creating unique excitation-emission spectra which can be used for precise identification. By using the spectral fingerprint measured, we aim to develop a novel technique using remote sensing. The experimental results presented a significant contribution to plastic and microalgal detection in surface waters by our developed LD-based fluorescence lidar system. Our fluorescence lidar system using a pulsed LD with excitation wavelength at 405 nm showed promising results in providing fluorescence lidar signal of several plastics. It reports the use of a fluorescence lidar system in real-time monitoring of microplastics and microalgae in different water systems. With the unique characteristic of phytoplankton in surface waters (Cadondon et al., 2024), we can distinguish plastics through their fluorescence characteristics (Fig. 4) with varying chemical composition.

Most studies use visual inspection through the camera, naked eye, and microscopy to identify photoluminescent plastics. However, transparent plastics are detected slowly. Among the examined plastic samples (Figs. 2 and 3), the highest fluorescence intensity signal was the PET plastic samples, easily detectable in real scenarios. On the other hand, the most abundant plastics are PS and PP (Koelmans et al., 2019), which have lower fluorescence intensity when excited at 405 nm. The water Raman signal also affects the low detection, and the CDOM content is also found in the surface waters. Autofluorescence and LIF studies of plastics are commonly conducted using excitation sources emitted at shorter wavelengths ranging from 200 nm to 355 nm. These sources allow fluorescence detection from carbonyl groups, which are present in polymer-based plastics (Spizzichino et al., 2016). Future studies extend the need for a datable of all fluorescence signatures of all suspended particles in surface waters.

4.3. Conclusion and future plans

Our study provides information on the potential of a portable LD-based fluorescence lidar system in detecting submerged plastics in surface waters. The experimental results conducted in a controlled environment showed the capability of our system to understand the fluorescence signatures of several plastics submerged 10 cm from the water's surface. We also conducted simultaneous detection of plastics and *C. vulgaris* using our setup, which explains the fluorescence effects of Raman scattering and microalgae in detecting plastic debris. Our system's portable and robust design can help coastal monitoring and management affected by residential and industrial effluents. The degradation of plastics and detection of smaller plastics is critically important in determining the effects on the health and environment. Such smaller sizes produced during the degradation of plastics have become an increasing concern in recent years due to potential health risks. In the future, we plan to quantify the number of plastics in surface waters and provide real-time information on such degradation processes using our developed system. Further development on our fluorescence lidar system is needed to provide accuracy and assess plastic litter in natural waters.

CRediT authorship contribution statement

Jumar Cadondon: Writing – review & editing, Writing – original draft, Visualization, Software, Methodology, Investigation, Formal analysis, Conceptualization. **Edgar Vallar:** Writing – review & editing, Validation, Supervision, Investigation, Conceptualization. **Tatsuo Shiina:** Writing – review & editing, Writing – original draft, Validation, Supervision, Resources, Project administration, Methodology, Investigation, Funding acquisition, Conceptualization. **Maria Cecilia Galvez:** Writing – review & editing, Writing – original draft, Validation, Supervision, Project administration, Investigation, Funding acquisition, Conceptualization.

Declaration of competing interest

The authors declare that they have no known competing financial interests or personal relationships that could have appeared to influence the work reported in this paper.

Data availability

Data will be made available on request.

Acknowledgements

The researchers want to acknowledge financial and logistical support to De La Salle University, the University of the Philippines Visayas, Chiba University, and the DOST-ASTHRDP program. This work was also supported by JSPS KAKENHI Grant Numbers JP23K26339, JP23H01645, and JP19H02383. It was also supported by DLSU RGMO Project Title "Fluorescence Detection of Microplastics in Surface Waters" with Project No. 02 FR 1TAY23-1TAY24.

Appendix A. Supplementary data

Supplementary data to this article can be found online at https://doi.org/10.1016/j.marpolbul.2024.116842.

References

Alzhuhairi, M., Al-Ghaban, A., Almutalabi, S.N., 2016. Chemical recycling of polyethylene terephthalate (PET) as additive for asphalt. ZJPAS 28(20, 675–679.
Andriolo, U., Goncalves, G., Bessa, F., Sobral, P., 2020. Mapping marine litter on coastal dunes with unmanned aerial systems: a showcase on the Atlantic Coast. Sci. Total Environ. 736, 139632.
Armitage, S., Awty-Carroll, K., Clewly, D., Martinez-Vicente, V., 2022. Detection and classification of floating plastic litter using a vessel-mounted video camera and deep learning. Remote Sens. (Basel) 14, 3425. https://doi.org/10.3390/rs14143425.
Ashjar, N., Keshavarzi, B., Moore, F., Zarei, M., Busquets, R., Zebarjad, S.M., Mohammadi., 2023. Microplastics (MPs) distribution in surface sediments of the Freidounkenar Paddy Wetland. Environ. Pollut. 317, 120799 https://doi.org/10.1016/j.envpol.2022.120799.
Bassi, R., Dall'Osto, L., 2021. Dissipation of light energy absorbed in excess: the molecular mechanisms. Annu. Rev. Plant Biol. 72, 47–76. https://doi.org/10.1146/annurev-arplant-071720-015522.
Cadondon, J., Ong, P.M., Vallar, E., Shiina, T., Galvez, M.C., 2022. Chlorophyll-a pigment measurement of spirulina in algal growth monitoring using portable pulsed LED fluorescence lidar system. Sensors 8, 2940. https://doi.org/10.3390/s22082940.
Cadondon, J., Vallar, E., Shiina, T., Galvez, M.C., 2023. Real-time Cholorophyll-a pigment monitoring of *Chlamydomonas reinhardtii* in a controlled environment using pulsed LED fluorescnece LiDAR system. Photonics 10, 144. https://doi.org/10.3390/photonics10020144.
Cadondon, J., Caido, N.G., Galvez, M.C., Rempillo, O., Esmeria Jr., J., Vallar, E., 2024. Black carbon and PM0.49 characterization in Manila north harbour port, Metro Manila, Philippines. Environ. Adv. 16, 100526 https://doi.org/10.1016/j.envadv.2024.
Casabianca, S., Bellingeri, A., Capellacci, S., Sbrana, A., Russo, T., Corsi, I., Penna, A., 2021. Ecological implications beyond the ecotoxicity of plastic debris on marine phytoplankton assemblage structure and functioning. Environ. Poll. 290, 118101 https://doi.org/10.1016/j.envpol.2021.118101.
Chen, S., Chen, P., Ding, L., Pan, D., 2023. A new semi-analytical MC model for oceanic LIDAR inelastic signals. Remote Sens. (Basel) 15, 684. https://doi.org/10.3390/rs15030684.

Churnside, J.H., Thorne, R.E., 2005. Comparison of airborne lidar measurements with 420 KHz echo-sounder measurements of zooplankton. Appl. Optics 44, 5504–5511.
Circelli, L., Cheng, Z., Garwood, E., Yuksel, K., Di Iorio, E., Angelico, R., Colombo, C., 2024. Comparison of ATR-FTIR and NIR spectroscopy for identification of microplastics in biosolids. Sci. Tot. Environ. 916, 170215 https://doi.org/10.1016/j.scitotenv.2024.170215.
Duan, J., Bola, N., Li, Y., Ding, S., Atugoda, T., Vithanage, M., et al., 2021. Weathering of microplastics and interaction with other coexisting constituents in terrestrial and aquatic environments. Water Res. 196, 117011.
Dussud, C., Meistertzheim, A.L., Conan, P., Pujo-Pay, M., George, M., Fabre, P., et al., 2018. Evidence of niche partitioning among bacteria living on plastics, organic particles, and surrounding seawaters. Environ. Pollut. 236, 807–816. https://doi.org/10.1016/j.envpo.2017.12.027.
Evans, M., Ruf, C., 2021. Toward the detection and imaging of ocean microplastics with a spaceborne radar. IEEE Trans. Geosci. Remote Sens. 60, 1–9.
Falkowski, P.G., Kolber, Z., 1995. Variations in chlorophyll fluorescence yields in phytoplankton in the world oceans. Funct. Plant Biol. 22, 341–355.
Falkowski, P.G., Lin, H., Gorbunov, M.Y., 2017. What limits photosynthetic energy conversion efficiency in nature? Lessons from the oceans. Philos. Trans. R. Soc. Lond. B Biol. Sci. 372, 20160376. https://doi.org/10.1098/rstb.2016.0376.
Galgani, L., Loiselle, S.A., 2021. Plastic pollution impacts on marine carbon biogeochemistry. Environ. Pollut. 268, 115598 https://doi.org/10.1016/j.envpol.115598.
Garaba, S.P., Aitken, J., Slat, B., Dierssen, H.M., Lebreton, L., Zielinkski, O., Reisser, J., 2018. Sensing ocean plastics with an airborne hyperspectral shortwave infrared imager. Environ. Sci. Technol. 52, 11699–11707. https://doi.org/10.1021/acs.est.8b02855.
Geraeds, M., van Emmerik, T., de Vries, R., bin Ab Razak, M.S., 2019. Riverine plastic litter monitoring using unmanned aerial vehicles (UAVs). Remote Sens. (Basel) 11, 2045. https://doi.org/10.3390/rs11172045.
Goddijn-Murphy, L., Peters, S., van Sebille, E., James, N.A., Gibb, S., 2018. Concept for a hyperspectral remote sensing algorithm for floating marine macro plastics. Mar. Pollut. Bull. 126, 255–262. https://doi.org/10.1016/j.marpolbul.2017.11.011.
Goddijn-Murphy, L., Martínez-Vicente, V., Dierssen, H.M., Raimondi, V., Gandini, E., Foster, R., Chirayath, V., 2024. Emerging technologies for remote sensing of floating and submerged plastic litter. Remote Sens. (Basel) 16 (10), 1770.
Hale, R.C., Song, B., 2020. Single-use plastics and COVID-19: scientific evidence and environmental regulations. Environ. Sci. Technol. 54, 7034–7036.
Koelmans, A.A., Mohamed Nor, N.H., Hermsen, E., Kooi, M., Mintenig, S.M., de France, J., 2019. Microplastics in freshwaters and drinking water: critical review and assessment of data quality. Water Res. 155, 410–422.
Lin, L., Yang, H., Xu, X., 2022. Effects of water pollution on human health and disease heterogeneity: a review. Front. Environ. Sci. 10, 880246 https://doi.org/10.3389/fenvs.2022.880246.
Lionetto, F., Lionetto, M.G., Mele, C., Corcione, C.E., Bagheri, et al., 2020. Authofluorescence of model polyethylene terephthalate nanoplastics cell interaction studies. Nanomaterials 12, 1560. https://doi.org/10.3390/nano12091560.
Loder, M.G.J., Gerdts, G., 2015. Methodology used for the detection and identification of microplastics – a critical appraisal. In: Bergmann, M., Gutow, L., Klages, M. (Eds.), Marine Anthropogenic Litter. Springer, Cham. https://doi.org/10.1007/978-3-319-16510-3_8.
Mace, T.H., 2011. At-sea detection of marine debris: overview of technologies, processes, issues, and options. Mar. Pollut. Bull. 65, 23–27. https://doi.org/10.1016/j.mar.po.bul.2011.08.042.
MacLeod, M., Arp, H.P.H., Tekman, M.B., Jahnke, A., 2021. The global threat from plastic pollution. Science 373, 61–65.
Mahmoud, A., El-Sharkawy, Y.H., 2024. Instant plastic waste detection on shores using laser-induced fluorescence and associated hyperspectral imaging. Opt. Quant. Electron. 56, 780. https://doi.org/10.1007/s11082-024-06564-8.
Mai, L., Bao, L.J., Shi, L., Wong, C.S., Zeng, E.Y., 2018. A review of methods for measuring microplastics in aquatic environments. Environ. Sci. Pollut. Res. Int. 25, 11319–11332. https://doi.org/10.1007/s11356-018-1692-0.
Mallory, M.L., Baak, J., Gjerdrum, C., Mallory, O., Manley, B., Swan, C., Provencher, J.F., 2021. Anthropogenic litter in marine waters and coastlines of Arctic Canada and West Greenland. Sci. Tot. Environ. 783, 146971 https://doi.org/10.1016/j.scitotenv.2021.146971.
Martinez-Vicente, V., Clark, J.R., Corradi, P., Aliani, S., Arias, M., Bochow, M., et al., 2019. Measuring marine plastic debris from space: initial assessment of observation requirements. Remote Sens. (Basel) 11, 2443. https://doi.org/10.3390/rs11202443.
Maslov, N.A., Dulin, V.M., 2020. Investigation of fluorescence spectra of various types of plastic for the purpose of sorting and further processing. J. Phys. Conf. Ser. 1677, 012185.
Maximenko, N., Corradi, P., Law, K.L., Sebille, E.V., Garaba, S.P., et al., 2019. Toward the integrated marine debris observing system. Front. Mar. Sci. 6, 447. https://doi.org/10.3389/fmrs.2019.00447.
Measures, R.M., 1984. Laser Remote Sensing: Fundamental and Applications. Wiley-Interscience, New York, NY, USA.
Meng, J., Zhang, Q., Zheng, Y., He, G., Shi, H., 2021. Plastic waste as the potential carriers of pathogens. Curr. Opin. Food Sci. 41, 224–230. https://doi.org/10.1016/j.cofs.2021.04.016.
Mikulec, V., Adamovic, P., Cvetkovic, Z., Ivesic, M., Kljusuric, J.G., 2023. Green techniques for detecting microplastics in marine emphasis on FTIR and NIR spectroscopy – short review. Processes 11, 2360. https://doi.org/10.3390/pr11082360.
NaRiKa, n.d. Plastic Sample B. Retrieved from http://dev-rika.narika.jp/ (accessed 20 May 2024).
Palmer, S.C.J., Pelevin, V.V., Goncharenko, I., Kovacs, A.W., Zlinsky, A., et al., 2013. Ultraviolet fluorescence LiDAR (UFL) as a measurement tool for water quality parameters in turbid lake conditions. Remote Sens. (Basel) 5, 4405–4422. https://doi.org/10.3390/rs5094405.
Palombi, L., Raimondi, V., 2022. Experimental tests for fluorescence LIDAR remote sensing of submerged plastic marine litter. Remote Sens. (Basel) 14, 5914. https://doi.org/10.3390/rs14235914.
Pang, X., Ren, L., Wu, S., Ma, W., Yang, J., Di, L., et al., 2020. Cold-chain food contamination as the possible origin of COVID-19 resurgence in Beijing. Nat. Sci. Rev. 7, 1861–1864.
Park, Y.-J., Garaba, S., Sainte-Rose, B., 2021. Detecting great Pacific garbage patch floating plastic litter using WorldView-3 satellite imagery. Opt. Express 29, 35288. https://doi.org/10.1364/OE.440380.
Povrozin, Y., Barbieri, B., 2016. Fluorescence Spectroscopy in *Handbook of Measurement in Science and Engineering*. John Wiley and Sons.
Rapa, M., Carstea, E.M., Saulean, A.A., Popa, C.L., Matei, E., Predescu, A.M., Predescu, C., Dontu, S.I., Dinca, A.G., 2024. An overview of the current trends in marine plastic litter management for a sustainable development. Recycling 9 (2), 30. https://doi.org/10.3390/recycling9020030.
Rogers, S.R., Webster, T., Livingstone, W., O'Drsicoll, N.J., 2012. Airborne laser-induced fluorescence (LIF) light detection and ranging (LiDAR) for the quantification of dissolved organic matter concentration in natural waters. Estuar. Coasts 35, 959–975.
Saito, Y., Takano, K., Kobayashi, F., Kobayashi, K., Park, H.-D., 2014. Development of a UV laser induced fluorescence lidar for monitoring blue-green algae in Lake Suwa. Appl. Optics 53, 7030–7036.
Santabarbara, S., Remelli, W., Petrova, A.A., Casazza, A.P., 2020. Influence of the wavelength of excitation and fluorescence emission detection on the estimation of fluorescence-based physiological parameters in different classes of photosynthetic organisms. In: Fluorescence Methods for Investigation of Living Cells and Microorganisms. IntechOpen, Rijeka, Croatia.
Shangguan, M., Liao, Z., Guo, Y., 2024. Simultaneous sensing profiles of beam attenuation coefficient and volume scattering function at 180o using a single-photon underwater elastic-Raman lidar. Opt. Exp. 32, 8189–8204. https://doi.org/10.1364/OE.5095596.
Shiina, T., 2019. LED mini lidar for atmospheric application. Sensors 19, 569. https://doi.org/10.3390/s19030569.
Shiina, T., 2020. Atmosphere Activity Measurement by LED Raman Mini Lidar, 237. EPJ Web Conferences, p. 07002.
Spizzichino, V., Caneve, L., Colao, F., Ruggiero, L., 2016. Characterization and discrimination of plastic materials using laser-induced fluorescence. Appl. Spectrosc. 70 (6) https://doi.org/10.1177/0003702816641267.
Strand, K.O., Huserbraten, M., Dagestad, K.-F., Mauritzen, C., et al., 2021. Potential sources of marine plastic from survey beaches in the Arctic and Northeast Atlantic. Sci. Total Environ. 790, 148009 https://doi.org/10.1016/j.scitotenv.2021.148009.
Veettil, B.K., Quan, N.H., Hauser, L.T. Doan, Van, D., Quang, N.X., 2022. Coastal and marine plastic litter monitoring using remote sensing: a review. Estuar. Coast. Shelf Sci. 279, 108160.
Vianello, A., Boldrin, A., Guerriero, P., Moschino, V., Rella, R., Sturaro, A., Da Ros, L., 2013. Microplastic particles in sediments of lagoon of Venice, Italy: first observations on occurrence, spatial patterns and identification. Estuar. Coast. Shelf Sci. 130, 54–61. https://doi.org/10.1016/j.ecss.2013.03.022.
Wagner, M., Scherer, C., Alvarez-Munoz, D., Brennholt, N., Bourrain, X., Buchinger, S., et al., 2014. Microplastics in freshwater ecosystems: what we know and what we need to know. Environ. Sci. Eur. 26, 12. https://doi.org/10.1186/s12302-014-0012-7.
Wohlschlager, M., Versen, M., 2020. Detection of plastics in water based on their fluorescence behavior. J. Sens. Sens. Syst. 9, 337–343. https://doi.org/10.5194/jsss-9-337-2020.
World Health Organization, 2019. Microplastics in Drinking Water. World Health Organization, Geneva Switzerland (ISBN 978-92-4-151619-8.).
Zhao, Y., Long, J., Zhuang, P., Ji, Y., He, C., Wang, H., 2022. Transforming polyethylene and polypropylene into nontraditional fluorescent polymers by thermal oxidation. J. Mater. Chem. C 10, 1010–1016. https://doi.org/10.1039/D1TC05520H.
Zhou, F., Wang, X., Wang, G., Zuo, Y., 2022. A rapid method for detecting microplastics based on fluorescence lifetime imaging technology (FLIM). Toxics 10, 118. https://doi.org/10.3390/toxics10030118.